Divergent roles of Smad3 and PI3-kinase in murine adriamycin nephropathy indicate distinct mechanisms of proteinuria and fibrogenesis

Published in final edited form as:
Kidney Int. 2012 September ; 82(5): 525–536. doi:10.1038/ki.2012.139.

Divergent roles of Smad3 and PI3-kinase in murine adriamycin nephropathy indicate distinct mechanisms of proteinuria and fibrogenesis

Gal Finer[1], **H. William Schnaper**[1], **Yashpal S. Kanwar**[2], **Xiaoyan Liang**[1], **Herbert Y. Lin**[3], and **Tomoko Hayashida**[1]

[1]Division of Kidney Diseases and Children's Memorial Research Center, Children's Memorial Hospital, Chicago, IL; and Department of Pediatrics, Northwestern University Feinberg School of Medicine, Chicago, IL

[2]Department of Pathology, Northwestern University Feinberg School of Medicine, Chicago, IL

[3]Department of Medicine, Center for Systems Biology, Program in Membrane Biology, Division of Nephrology, Massachusetts General Hospital and Harvard Medical School, Boston, MA

Abstract

Multiple transforming growth factor (TGF)-β-induced fibrogenic signals have been described *in vitro.* To evaluate mechanisms *in vivo*, we used an adriamycin nephropathy model in 129x1/Svj mice that display massive proteinuria by day 5 to7 and pathological findings similar to human focal segmental glomerulosclerosis by day 14. TGF-β mRNA expression increased after day 7 along with nuclear translocation of the TGF-β receptor-specific transcription factor Smad3. Inhibiting TGF-β prevented both pathological changes and type-I collagen and fibronectin mRNA expression, but proteinuria persisted. Renal Akt was phosphorylated in adriamycin-treated mice, suggesting PI3-kinase activation. Expression of mRNA for the p110γ isozyme of PI3-kinase was specifically increased and p110γ colocalized with nephrin by immunohistochemistry early in disease. Nephrin levels subsequently decreased. Inhibition of p110γ by AS605240 preserved nephrin expression and prevented proteinuria. In cultured podocytes, adriamycin stimulated p110γ expression. AS605240, but not a TGF-β receptor kinase inhibitor, prevented adriamycin-induced cytoskeletal disorganization and apoptosis, supporting a role for p110γ in podocyte injury. AS605240, at a dose that decreased proteinuria, prevented renal collagen mRNA expression *in vivo* but did not affect TGF-β-stimulated collagen induction *in vitro*. Thus, PI3-kinase p110γ mediates initial podocyte injury and proteinuria, both of which precede TGF-β-mediated glomerular scarring.

Keywords

TGF-β; glomerulosclerosis; Cell Signaling; podocyte; fibrosis

Introduction

Renal fibrosis is a complex process involving multiple cell types and a broad variety of mediators. Podocyte injury is one of the initial steps in the sequence leading to

Corresponding author: Tomoko Hayashida, MD, PhD, 310 E Superior St, Morton 4-685, Chicago, IL 60611, Fax: 312-503-1181, Tel: 312-503-0089, hayashida@northwestern.edu.

Disclosure
All the authors declared no competing interests.

glomerulosclerosis and subsequent renal scarring (1, 2). Misdirected attempts at tissue repair then involve numerous other cells in scar formation (3). Multiple studies have implicated transforming growth factor (TGF)-β as a pivotal cytokine that promotes both physiological healing and pathological scarring, including in the kidney (4–7). We previously showed that TGF-β activates type-I collagen expression in cultured kidney mesangial and epithelial cells via a complex signaling mechanism in which the classical TGF-β/Smad pathway is regulated by a number of non-canonical pathways involving ERK MAP kinase (8), phosphatidylinositol-3-kinase (PI3K) (9), protein kinase CδE(10) and the Rho-family GTPases (11, 12). In diabetes, TGF-β has been shown to interact with PI3K to promote mesangial cell dysfunction (13, 14). TGF-β-PI3K cross talk also was demonstrated to be important in renal epithelial-to-mesenchymal transition in vitro and in vivo (15).

The present study was aimed at elucidating the involvement of TGF-β and PI3K in an animal model of acquired kidney fibrosis. Adriamycin (ADR)-induced kidney damage is one of the few existing murine models of acquired glomerulonephropathy (16) in which progressive renal changes lead to terminal renal failure (17). By a mechanism that is not completely understood, ADR induces pathological glomerular changes that are similar to human focal segmental glomerular sclerosis (FSGS) (18). TGF-β involvement in the ADR model has been suggested in earlier studies (5, 19). Some of the model's limitations include severity of the kidney injury and strain specificity - mostly restricted to Balb/c mice (20). A genome-wide search linked strain susceptibility to anthracyclines to a specific genetic locus, which is shared between Balb/c and 129/SvJ, but not with C57BL6 mice (21, 22). Accordingly, we extended the ADR model to the 129x1/SvJ strain and observed that ADR indeed induces similar, but milder pathological changes than were seen in Balb/C strain of mice. We implicate TGF-β and the p110γ isoform of PI3K in the pathogenesis of this nephropathy model. Our data suggest that PI3K p110γ promotes podocyte injury resulting in proteinuria, via cell signaling that is not directly dependent on TGF-β/Smad3 pathway activation. Conversely, TGF-β/Smad3 signaling is not involved in proteinuria, but instead plays a significant part in consequent fibrogenesis. Our results define mechanisms underlying proteinuria and fibrogenesis in chronic kidney disease and indicate that these mechanisms are likely to be distinct.

Results

Characterization of ADR nephropathy in 129x1/Svj mice

Three to 5 days following tail-vein administration of one dose of ADR (15 mg/kg BW) to 129x1/Svj mice, albuminuria developed, and progressed to massive proteinuria and hypoalbuminemia during the second and third weeks of disease (Figures 1A and 1B). In addition, ADR-treated mice manifested hypercholesterolemia (Figure 1B, and Table 1). Renal dysfunction was mild initially, primarily with BUN elevation, but progressed to advanced kidney dysfunction with doubling of baseline serum creatinine about four weeks after ADR (Figure 1B). By light microscopy, kidneys of ADR-treated mice showed glomerular mesangial hypercellularity and extracellular matrix expansion accompanied with partially collapsed glomerular capillary loops. Two weeks following ADR administration, some of the glomeruli had segmental sclerosis/hyalinosis, while others showed proliferation of parietal epithelial cells reminiscent of cellular crescents. Global glomerular sclerosis with hyalinization of the entire glomerular tuft was observed as well. Influx of inflammatory cells into the interstitium, accompanied by interstitial edema, was also seen. Tubular atrophy followed, beginning at week 2 (Figure 1C) and progressing thereafter (not shown). At 2 weeks, mRNA expression of fibronectin and type I collagen in kidneys of ADR-treated mice increased up to15-fold (Figure 2A). At the same time, an increased amount of connective tissue in the glomerular and tubular compartments was observed, as assessed by trichrome

staining (Figure 2B, top panels). This was associated with increased type-I collagen expression, as demonstrated by immunohistochemistry (Figure 2B, bottom panels).

TGF-β mediates fibrogenesis in mouse ADR nephropathy

Using cell culture systems, we and others previously showed that TGF-β is an important mediator of renal fibrosis. Here, we examined TGF-β involvement in our model of acquired kidney fibrosis. Consistent with previous reports (5, 19), TGF-β1 mRNA levels were increased in ADR kidneys, peaking around the third week after the injurious stimulus and subsiding gradually thereafter (Figure 3A). The downstream mediator of TGF-β, Smad3, was phosphorylated and accumulated in nuclei of kidney tubular and glomerular cells in ADR-treated mice (Figure 3B), indicating that Smad3 is activated. To test whether TGF-β mediates fibrosis in this model, a soluble TGF-β type II receptor-Fc (sTβRII-Fc) was utilized. This chimeric protein previously has been shown to inhibit renal fibrosis in mouse diabetes (23). sTβRII-Fc decreased glomerulomegaly, glomerulosclerosis and crescent formation in ADR-treated mouse kidneys (Figure 4A and Table 2). Induction of type-I collagen, fibronectin and TGF-β1 mRNA after ADR administration was also attenuated by sTβRII-Fc (Figure 4B). Interestingly, albuminuria persisted, despite the improved glomerular fibrotic changes, with the sTβRII-Fc treatment (Figure 5A). Further, loss of podocyte markers caused by ADR, as determined by podocalyxin mRNA expression (Figure 5B) and by nephrin staining (Figure 5C), was not prevented by sTβRII-Fc. These results suggest that TGF-β mediates glomerular fibrosis but not podocyte injury and subsequent proteinuria in our model. Successful inhibition of the TGF-β/Smad pathway by the sTβRII-Fc was confirmed by reduction of Smad3 phosphorylation in the treated mouse kidneys (Figure 5D). Efficacy of the sTβRII-Fc was also confirmed in cultured HKC cells by inhibition of TGF-β-induced COL1A1 mRNA (data not shown).

PI3K isoform p110γ plays a role in ADR nephropathy

Previous work in our laboratory showed that PI3K activity is required for TGF-β-stimulated type-I collagen production in mesangial cells in culture (9). We therefore examined the role of PI3K in our mouse model of acquired nephropathy. PI3K activity, as determined by staining for phosphorylation of the downstream target protein Akt, was detectable in the ADR-treated mouse kidneys, in glomeruli and to a lesser extent in tubules (Figure 6A). Levels of mRNA were comparable for the most commonly described PI3K catalytic subunits, the ubiquitous isoforms α and β, as well as for their regulatory subunits. In contrast, the p110γ catalytic subunit isoform was specifically upregulated in the ADR kidney (Figure 6B). This finding was at first surprising to us, as the p110γ isoform is particularly highly expressed in lymphoid cells, with low-to-modest expression in other organs (24). To test if the upregulation of p110γ mRNA in the ADR kidney reflects its expression by kidney cells, rather than by infiltrating inflammatory cells, kidney sections were stained for p110γ, along with nephrin as a podocyte marker. p110γ staining was weakly positive in glomeruli of control mouse kidney, and became more obvious at days 3 and 6 after ADR administration (Figure 6C). The p110γ staining co-localized with nephrin, suggesting p110γ expression in podocytes. Of note, disruption of nephrin staining starts as early as day 3 after the ADR administration. The timing of podocyte marker loss and p110γ expression coincides with the onset of albuminuria, but precedes overt fibrotic changes.

To further assess a potential role for PI3Kγ in ADR nephropathy, we administered a specific inhibitor of p110γ, AS605240 (25), 30 mg/kg BW i.p. 1 day prior to ADR administration, followed by every-other-day injection. No significant animal, tissue or cell toxicity related to the use of AS605240 was observed during the 2-week period of the experiments. PI3K p110γ inhibition attenuated proteinuria that was induced by ADR (Figure 7A). AS605240 also decreased mRNA expression of type-I collagen and fibronectin

(Figure 7B), and fibrotic histological changes and collagen deposition (Figure 7C). Nephrin (protein) and podocalyxin (mRNA) expression were preserved in animals treated with AS605240 (Figure 7D and 7E), suggesting that in-vivo inhibition of p110γ protects against ADR-induced podocyte injury.

To determine how p110γ affects podocyte function, we examined its role in podocyte injury in culture. p110γ protein expression was detected by immunoblotting, and AS605240 (1 μM) reduced basal Akt activity in cultured podocytes, suggesting that the p110γ isoform is indeed expressed and contributes to downstream Akt activity in podocytes (Figure 8A). In comparison, TGF-β-stimulated Smad activity was not affected by the p110γ inhibitor (not shown). ADR treatment (20 μg/ml, 16 hrs) significantly increased p110γ mRNA expression in cultured podocytes (Figure 8B). ADR treatment induced podocyte apoptosis, as detected by expression of cleaved caspase 3 product (Figure 8C) and staining with an early apoptosis marker, cytoDEATH (Figure 8D, upper panels), and disorganization of the cytoskeletal stress fiber pattern (Figure 8E) that is seen normally in differentiated podocytes (26). These podocyte changes were prevented by pre-treatment with AS605240, supporting a role for PI3K p110γ in podocyte injury. In contrast, a TGF-β receptor kinase inhibitor, SB431542, did not affect podocyte apoptosis nor cytoskeletal disorganization by ADR. Further, ADR induced cleaved caspase 3 products even in a Smad3 −/− podocyte (Figure 8C, bottom panels). Together, these data, indicate that ADR-stimulated podocyte damage is mediated by PI3K p110γ, but independent of TGF-β in the time frame that we studied.

Distinct roles of PI3K p110γ and TGF-β and in kidney fibrosis

We next addressed a possible hierarchy between p110γ and TGF-β signaling in our model. The increased pAkt activity that we observed in ADR-treated mouse glomeruli (Figure 6) was not affected by sTβRII-Fc (Figure 9A). Conversely, ADR-stimulated TGF-β1 mRNA expression in mouse kidneys was prevented by treatment with the p110γ inhibitor (Figure 9B). These results suggest that p110γ activation and podocyte injury precede the induction of TGF-β expression. In culture, podocytes express little type I collagen mRNA both basally and in response to TGF-β1 (data not shown), and TGF-β1 treatment did not change p110γ protein expression (Figure 9C). In the human kidney epithelial cell (HKC) line, the p110γ-specific PI3K inhibitor did not affect TGF-β induction of collagen mRNA expression (Figure 9D), whereas a general PI3K inhibitor that blocks all classes of PI3K including the ubiquitously expressed α and β isoforms, LY294002, abrogated the collagen response, as we have reported previously (9). Therefore, the PI3Kγ inhibitor did not ameliorate fibrosis by directly inhibiting glomerular collagen expression, but rather by preventing glomerular injury and suppressing subsequent production of a fibrogenic cytokine, TGF-β.

Discussion

In progressive renal failure, a final common pathway culminates in glomerulosclerosis and tubulointerstitial fibrosis, irrespective of the nature of the original disease. Understanding the molecular mechanisms that are involved is important for developing specific, effective treatments. Animal models of glomerulopathies have been used widely to study signaling pathways involved in the pathogenesis of renal fibrosis. Previous studies suggested that injury to podocytes, essential elements in maintaining glomerular filtration barrier integrity, is the initiating cause of many genetic (27) and acquired--both primary and secondary (3, 28, 29)--renal diseases. In the present paper, we describe a modified version of a previously established rodent model of ADR nephropathy (17, 30) and utilize it to dissect renal fibrotic mechanisms. In 129x1/SvJ mice, proteinuria, chemical indices of nephrotic syndrome and glomerular and tubulointerstitial accumulation of type-I collagen and fibronectin occur sequentially after ADR administration. These changes are similar in nature and order to those of human FSGS. In contrast, preliminary experiments with Balb/c mice (not shown)

yielded a more diffuse and aggressive pattern of injury. We therefore propose that the present model offers a pattern of injury and response more representative of human, progressive glomerulosclerosis.

In evaluating non-canonical TGF-β signaling that we previously described *in vitro*, we found increased Akt activity in both Balb/c and 129x1/SvJ kidneys after ADR treatment. We were surprised that only the γ isoform of PI3K showed increased expression. PI3K p110γ is highly enriched in leukocytes but also is expressed in cardiomyocytes, endothelial cells, pancreatic islets and smooth muscle cells (24, 31–33). The likely source of this isoform in our model is the podocyte, since p110γ colocalizes with nephrin in mouse glomeruli, and cultured podocytes express this isoform.

Intact actin cytoskeletal structure is essential for the maintenance of effective foot-processes morphology and normal podocyte function (2), and PI3K-dependent Akt activity has been shown to regulate this structure (34). Since we previously showed that a pan-PI3K inhibitor, LY294002 blocked TGF-β1 induction of type I collagen expression in cultured renal cells (9), we evaluated the effect of LY294002 in vivo. Our results were inconclusive; some mice that survived showed histological amelioration of ADR nephropathy whereas others died from possible toxicity or even from exacerbation of the disease. Of note, treatment with LY294002 alone consistently increased urine albumin compared to negative control mice (data not shown). On the other hand, specific blockade of the p110γ isoform of PI3K with AS605240 decreased proteinuria and fibrosis in ADR-treated mice, without affecting control mice. Further, inhibiting p110γ activity in cultured podocytes using AS605240 decreased ADR-stimulated cytoskeletal disorganization and induction of apoptotic markers in cultured cells. Together, these data suggest that p110γ plays a significant role in mediating podocyte injury at the initiation of the disease process. In contrast, AS605240 did not inhibit TGF-β-stimulated collagen expression in cultured cells, indicating that p110γ does not directly mediate TGF-β-stimulated fibrogenesis. Further, ADR-increased renal expression of TGF-β was partially blocked by the p110γ inhibitor in vivo, suggesting that p110γ activity precedes TGF-β expression and consequent collagen production. Consistent with this hypothesis, sTβRII-Fc did not prevent either glomerular pAkt activity induced by PI3K p110γ in vivo or ADR-induced podocyte damage in vitro.

These findings suggest that PI3K p110γ is a novel therapeutic target mediating podocyte injury. While the α and β isoforms of PI3K are ubiquitously expressed and the most well studied, they are activated primarily by a receptor tyrosine kinase. The γ isoform, which is relatively restricted to hematopoietic cells, is uniquely activated by G-protein-coupled receptor agonists. Due to its tissue distribution, specific roles for the γ isoforms were preferentially evaluated in inflammatory and/or autoimmune disease models such as asthma and systemic lupus erythematosus, and determined to play a role in immune cell function (25, 35, 36). Given the potential role of p110γ in inflammation, we cannot rule out the possibility that p110γ inhibition ameliorates disease progression in part through an anti-inflammatory mechanism. Nonetheless, our data are consistent with a model in which PI3K P110γ plays an important role specifically in podocyte injury.

TGF-β is generally accepted as a central mediator in kidney fibrosis (reviewed in (7) and references therein). Its fibrogenic properties are supported by a transgenic mouse model of TGF-β overexpression (37) and by subsequent studies in several animal models of kidney fibrosis. Our results show that extracellular matrix expression in ADR mouse kidney was mediated by TGF-β, as indicated by increased expression of TGF-β, Smad3 phosphorylation, nuclear translocation of Smad3 and amelioration of disease manifestations by sTβRII-Fc. Since p110γ activity occurs prior to TGF-β expression, prevention of fibrotic marker expression in ADR-treated mouse kidneys by AS605240 likely represents blockade

of the events initiating the disease rather than direct interference with a TGF-β-mediated mechanism. Conversely, s-TβRIIFc decreased fibrosis but did not prevent proteinuria. Together, our results define distinct and sequential roles of p110γ and TGF-β, the former as an initial stress response to ADR leading to podocyte injury, proteinuria and TGF-β expression, and the latter contributing to subsequent extracellular matrix accumulation. Other isoforms of PI3K, probably α and/or β, likely interfere with signaling downstream from TGF-β, as we previously showed in vitro (9). The proposed signaling cascade involving PI3K and TGF-β is depicted as a diagram (Figure 10). The sequence of events that we propose is supported by the following observations: (1) proteinuria precedes fibrosis; (2) ADR-stimulated changes in podocyte function that are consistent with causal events in proteinuria are blocked by AS605240; (3) p110γ antagonism prevents both proteinuria and fibrosis; and (4) sTβRII-Fc ameliorates fibrosis but not proteinuria.

One of the main advantages of our model in 129x1/SvJ is the nature of the histological lesion, which differs from the more aggressive tissue damage observed in Balb/c mice ((5, 17, 19, 30) and our unpublished results). Thus results from the current model may reflect a series of events from an earlier stage of the disease than those observed in Balb/c. We note that the lesion in this model is not purely glomerular, and dilated tubules and tubulointerstitial fibrosis are also prominent. However, the initial podocyte damage and sustained proteinuria suggest that the model represents a primary glomerular process that, in an accelerated manner, invokes the same mechanisms of disease progression that are observed in human FSGS. Further understanding of the molecular mechanisms underlying progression of chronic kidney disease is crucial for successful treatment. Additional studies will help us apply experimental evidence to patient therapy.

Materials and Methods

Animal Model

Animal experiments were performed in accordance with the regulations set by the institutional committee for the care and use of laboratory animals. Male 129x1/SvJ mice of 6–8 weeks of age weighing 24–26 g (Jackson laboratory, Bar Harbor, ME) were fed a standard laboratory diet and provided with water ad libitum. Disease was induced by a single intravenous injection of ADR, 15 mg/kg (Research Product International, Mt. Prospect, IL), in 0.9% saline. Control mice received the same volume of saline. Soluble type II TGF-β receptor antagonist (sTβRII-Fc), produced by H. Lin (23), was injected intravenously (4 mg/kg) a day prior to ADR injection, followed by intraperitoneal injections (2 mg/kg) twice weekly thereafter for a total of 5 doses. A p110γ-specific inhibitor, AS605240 (EMD chemicals, Gibbstown, NJ), was reconstituted in DMSO for stock solution and further diluted with 0.9% saline before each injection. 30mg/kg p110γ inhibitor was administered intraperitoneally starting the day prior to ADR injection and every other day thereafter. Before sacrifice, 24-h urine samples were collected in a metabolic cage. Blood samples were taken by cardiac puncture after anesthesia. The kidneys were rapidly removed and preserved in halves for later processing for protein, mRNA, histology, and immunofluorescence studies.

Renal histopathology

Specimens were fixed in 10% neutral buffered formalin, and paraffin-embedded and sectioned (4 μm thick) by Northwestern University Mouse Histology and Phenotyping Laboratory. Periodic Acid-Schiff (PAS) and Masson's Trichrome staining (Accustain, Sigma, St Louis, MO), were performed according to the manufacturer's instruction. The stained sections were coded and examined by two independent observers who were blinded to the treatment groups. The histological changes for segmental glomerulosclerosis, tubular

dilatation, protein cast deposition inside the tubules and interstitial fibrosis were evaluated semiquantitatively by a scoring system of 0–3, where 0 = no change; 1 = mild change, 2 = moderate; 3 = severe.

Immunohistochemical analysis

Formalin-fixed, paraffin-embedded, 4-μm sections were prepared and mounted on glass slides, deparaffinized, rehydrated and then subjected to antigen retrieval following the vendor's instructions (DAKO, Carpinteria, CA). The sections were incubated with 3% H_2O_2 to quench endogenous peroxidase activity. After treating with a blocking solution (Power Block, BioGenex, San Ramon, CA), the sections were incubated with primary antibody in a diluent (DAKO) overnight. The bound antibody was detected by peroxidase-conjugated secondary antibody and visualized with DAB substrate (Invitrogen, Carlsband, CA), followed by Hematoxylin counterstaining. For immunofluorescence microscopy, freshly frozen 1–2 mm slices of kidney tissues were fixed with 4% paraformaldehyde at 4°C overnight. They were embedded in 30% sucrose/1.5% agarose and 10 μm-thick cryosections were prepared using Leica CM1850 Cryotome (Leica Microsystems), followed by standard immunostaining procedures. Antibodies isotype-matched to the primary antibodies were used as negative controls. Images were captured using an Axioscope equipped with UV epi-illumination or Zeiss LSM 510 META laser scanning confocal microscope (Zeiss, Thornwood, NY).

Determination of mouse urinary protein excretion and serum biochemistry

Albuminuria was measured using an Albuwell ELISA kit (Exocell, Philadelphia, PA) according to the manufacturer's protocol. Mouse serum was analyzed for albumin, cholesterol, creatinine and blood urea nitrogen (BUN) by Charles River Laboratories (Wilmington, MA).

Evaluation of mRNA expression

Total RNA was extracted from tissue preserved with RNAlater using the RNeasy mini kit with DNase (Qiagen, Valencia, CA) as instructed by the manufacturer. 1 μg of RNA, quantified with the Quant-it RiboGreen assay (Invitrogen), was reverse-transcribed with the iScript cDNA synthesis kit (Bio-Rad Laboratories), and subjected to quantitative PCR using the iQ SYBR Green Supermix (Bio-Rad Laboratories) with the iCycler iQ real-time PCR detection system (Bio-Rad). Real-time data were collected for 40 cycles of 95 °C, 10 s, 57 °C, 45 s, and 75 °C, 30 s. Primers used are custom-synthesized by either Integrated DNA Technology (Coralville, CA) or Invitrogen. Relative expression of the gene of interest was estimated by the ΔΔCt method using 18S or β2-microglobulin as a reference gene. Samples were analyzed in triplicate, and experiments were repeated at least three times. Detailed primer information is attached as Table A in the supplementary data.

In vitro studies

Cell culture and treatment—Mouse podocytes were kindly provided by Dr E. Bottinger (38) and maintained as previously described (26). Briefly, cells were propagated in a permissive condition (33°C) with RPMI1640 supplemented with 10% heat-inactivated FBS, IFNγ (20U/ml, Cell Sciences, Canton, MA) on dishes coated with rat type I collagen (BD Biosciences, Bedford, MA). Differentiation was induced in the absence of IFNγ at 37°C for at least 2 weeks. The human renal tubular epithelial cell line HKC, generously gifted by Dr. L. Racusen (39), was cultured in Dulbecco's modified Eagle's medium/F-12 supplemented with 10% FBS, penicillin/streptomycin, amphotericin B, Hepes buffer, and glutamine.

Preparation of cell lysate and western blot analysis—Cells were lysed on ice in RIPA buffer (50 mM Tris/HCl, pH 7.5; 150 mM NaCl; 1% Nonidet P-40; 0.5% deoxycholate; 0.1% SDS) containing protease and phosphatase inhibitor cocktails (Sigma). Protein samples were subjected for immunoblotting and immunoreactive bands were visualized by chemiluminescence reagent according to the manufacturer's protocol (Santa Cruz Biotechnology).

Immunocytochemistry—Cells were plated on gelatin-coated glass cover slips and immunostained with a standard protocol and examined by Zeiss LSM 510 meta confocal microscope as previously described (40). Early apoptosis was detected by M30 CytoDEATH (Roche applied bioscience, Indianapolis, IN).

Antibodies and reagents—Primary antibodies were purchased as follows; nephrin (R & D systems, Minneapolis, MN), pSmad3 (Ser 425) and p110γ (Abcam, Cambridge, MA), pAkt (Ser 473) and Akt (Cell Signaling, Danvers, MA), type I collagen (Fitzgerald, Concord, MA), Rhodamine-Phalloidin (Cytoskeleton, Denver CO) and secondary antibodies; NorthernLight-conjugated secondary antibodies (R & D), Alexa-conjuaged secondary antibodies (Invitrogen), peroxidase-conjuaged secondary antibodies (Abcam or Invitrogen). TGF-β1 (R & D) was reconstituted as previously described and used at the final concentration of 1.0 ng/ml (8). SB431542 and AS605240 were purchased from EMD biochemicals and reconstituted in DMSO.

Statistical Analysis

Statistical analyses were performed using GraphPad Prism version 4.0 for Macintosh (GraphPad Software, San Diego, CA) for Students' *t* test or 1- or 2-way analysis of variance followed by Fisher's post-hoc analysis. $P < 0.05$ was considered significant.

Supplementary Material

Refer to Web version on PubMed Central for supplementary material.

Acknowledgments

Supported in part by Grants R01-DK049362, R01-DK075663 (H.W.S.), R01-DK060635 (Y.K) and R01-DK069533 AND R01-DK071837 (H.Y.L.). Dr. Finer was the recipient of an Amgen Fellowship.

The Cell Imaging Facility and Mouse Histology and Phenotyping Laboratory of the Northwestern University are supported by NCI CCSG P30 CA060553 awarded to the Robert H Lurie Comprehensive Cancer Center.

We thank members of the Schnaper lab for helpful discussions.

References

1. Barisoni L, Schnaper HW, Kopp JB. A proposed taxonomy for the podocytopathies: a reassessment of the primary nephrotic diseases. Clin J Am Soc Nephrol. 2007; 2:529–42. [PubMed: 17699461]
2. Mundel P, Reiser J. Proteinuria: an enzymatic disease of the podocyte? Kidney Int. 2010; 77:571–80. [PubMed: 19924101]
3. Schnaper HW, Hubchak SC, Runyan CE, et al. A conceptual framework for the molecular pathogenesis of progressive kidney disease. Pediatr Nephrol. 2010; 25:2223–30. [PubMed: 20352456]
4. Yamamoto T, Noble NA, Miller DE, et al. Sustained expression of TGF-β1 underlies development of progressive kidney fibrosis. Kidney Int. 1994; 45:916–27. [PubMed: 8196298]
5. Tamaki K, Okuda S, Ando T, et al. TGF-β1 in glomerulosclerosis and interstitial fibrosis of adriamycin nephropathy. Kidney Int. 1994; 45:525–36. [PubMed: 8164441]

6. Bottinger EP, Bitzer M. TGF-β signaling in renal disease. J Am Soc Nephrol. 2002; 13:2600–10. [PubMed: 12239251]
7. Schnaper HW, Jandeska S, Runyan CE, et al. TGF-β signal transduction in chronic kidney disease. Front Biosci. 2009; 14:2448–65. [PubMed: 19273211]
8. Hayashida T, Decaestecker M, Schnaper HW. Cross-talk between ERK MAP kinase and Smad signaling pathways enhances TGF-β-dependent responses in human mesangial cells. FASEB J. 2003; 17:1576–8. [PubMed: 12824291]
9. Runyan CE, Schnaper HW, Poncelet AC. The phosphatidylinositol 3-kinase/Akt pathway enhances Smad3-stimulated mesangial cell collagen I expression in response to transforming growth factor-β1. J Biol Chem. 2004; 279:2632–9. [PubMed: 14610066]
10. Runyan CE, Schnaper HW, Poncelet AC. Smad3 and PKCδ mediate TGF-β1- induced collagen I expression in human mesangial cells. Am J Physiol Renal Physiol. 2003; 285:F413–22. [PubMed: 12759229]
11. Hubchak SC, Runyan CE, Kreisberg JI, et al. Cytoskeletal rearrangement and signal transduction in TGF-β1-stimulated mesangial cell collagen accumulation. J Am Soc Nephrol. 2003; 14:1969–80. [PubMed: 12874450]
12. Hubchak SC, Sparks EE, Hayashida T, et al. Rac1 promotes TGF-β-stimulated mesangial cell type I collagen expression through a PI3K/Akt-dependent mechanism. Am J Physiol Renal Physiol. 2009; 297:F1316–23. [PubMed: 19726546]
13. Kato MYH, Xu ZG, Lanting L, Li SL, Wang M, Hu MC, Reddy MA, Natarajan R. Role of the Akt/FoxO3a pathway in TGF-β1-mediated mesangial cell dysfunction: a novel mechanism related to diabetic kidney disease. J Am Soc Nephrol. 2006; 17:3325–35. [PubMed: 17082237]
14. Reeves WBAT. Transforming growth factor β contributes to progressive diabetic nephropathy. Proc Natl Acad Sci U S A. 2000; 97:7667–9. [PubMed: 10884396]
15. Kattla JJ, Carew RM, Heljic M, et al. Protein kinase B/Akt activity is involved in renal TGF-β1-driven epithelial-mesenchymal transition in vitro and in vivo. Am J Physiol Renal Physiol. 2008; 295:F215–25. [PubMed: 18495798]
16. Fogo AB. Animal models of FSGS: lessons for pathogenesis and treatment. Semin Nephrol. 2003; 23:161–71. [PubMed: 12704576]
17. Okuda S, Oh Y, Tsuruda H, et al. Adriamycin-induced nephropathy as a model of chronic progressive glomerular disease. Kidney Int. 1986; 29:502–10. [PubMed: 3486312]
18. Yasuda K, Park HC, Ratliff B, et al. Adriamycin nephropathy: a failure of endothelial progenitor cell-induced repair. Am J Pathol. 2010; 176:1685–95. [PubMed: 20167859]
19. Li J, Campanale NV, Liang RJ, et al. Inhibition of p38 mitogen-activated protein kinase and transforming growth factor-β1/Smad signaling pathways modulates the development of fibrosis in adriamycin-induced nephropathy. Am J Pathol. 2006; 169:1527–40. [PubMed: 17071578]
20. Lui SL, Tsang R, Chan KW, et al. Rapamycin attenuates the severity of murine adriamycin nephropathy. Am J Nephrol. 2009; 29:342–52. [PubMed: 18948688]
21. Zheng Z, Schmidt-Ott KM, Chua S, et al. A Mendelian locus on chromosome 16 determines susceptibility to doxorubicin nephropathy in the mouse. Proc Natl Acad Sci U S A. 2005; 102:2502–7. [PubMed: 15699352]
22. Papeta N, Zheng Z, Schon EA, et al. Prkdc participates in mitochondrial genome maintenance and prevents Adriamycin-induced nephropathy in mice. J Clin Invest. 2010; 120:4055–64. [PubMed: 20978358]
23. Russo LM, del Re E, Brown D, et al. Evidence for a role of transforming growth factor-β1 in the induction of postglomerular albuminuria in diabetic nephropathy: amelioration by soluble TGF-beta type II receptor. Diabetes. 2007; 56:380–8. [PubMed: 17259382]
24. Ohashi PS, Woodgett JR. Modulating autoimmunity: pick your PI3 kinase. Nat Med. 2005; 11:924–5. [PubMed: 16145571]
25. Camps M, Ruckle T, Ji H, et al. Blockade of PI3Kγ suppresses joint inflammation and damage in mouse models of rheumatoid arthritis. Nat Med. 2005; 11:936–43. [PubMed: 16127437]
26. Mundel P, Reiser J, Kriz W. Induction of differentiation in cultured rat and human podocytes. J Am Soc Nephrol. 1997; 8:697–705. [PubMed: 9176839]

27. Benoit G, Machuca E, Heidet L, et al. Hereditary kidney diseases: highlighting the importance of classical Mendelian phenotypes. Ann N Y Acad Sci. 2010; 1214:83–98. [PubMed: 20969579]
28. Kumar PA, Brosius FC 3rd, Menon RK. The glomerular podocyte as a target of growth hormone action: implications for the pathogenesis of diabetic nephropathy. Curr Diabetes Rev. 2011; 7:50–5. [PubMed: 21067510]
29. Leeuwis JW, Nguyen TQ, Dendooven A, et al. Targeting podocyte-associated diseases. Adv Drug Deliv Rev. 2010; 62:1325–36. [PubMed: 20828590]
30. Wang Y, Wang YP, Tay YC, et al. Progressive adriamycin nephropathy in mice: sequence of histologic and immunohistochemical events. Kidney Int. 2000; 58:1797–804. [PubMed: 11012915]
31. Hirsch E, Lembo G, Montrucchio G, et al. Signaling through PI3Kγ: a common platform for leukocyte, platelet and cardiovascular stress sensing. Thromb Haemost. 2006; 95:29–35. [PubMed: 16543958]
32. Vanhaesebroeck B, Ali K, Bilancio A, et al. Signalling by PI3K isoforms: insights from gene-targeted mice. Trends Biochem Sci. 2005; 30:194–204. [PubMed: 15817396]
33. Kok K, Geering B, Vanhaesebroeck B. Regulation of phosphoinositide 3-kinase expression in health and disease. Trends Biochem Sci. 2009; 34:115–27. [PubMed: 19299143]
34. Zhu J, Sun N, Aoudjit L, et al. Nephrin mediates actin reorganization via phosphoinositide 3-kinase in podocytes. Kidney Int. 2008; 73:556–66. [PubMed: 18033240]
35. Barber DF, Bartolome A, Hernandez C, et al. PI3Kγ inhibition blocks glomerulonephritis and extends lifespan in a mouse model of systemic lupus. Nat Med. 2005; 11:933–5. [PubMed: 16127435]
36. Takeda M, Ito W, Tanabe M, et al. The pathophysiological roles of PI3Ks and therapeutic potential of selective inhibitors in allergic inflammation. Int Arch Allergy Immunol. 2010; 152 (Suppl 1): 90–5. [PubMed: 20523070]
37. Mozes MM, Bottinger EP, Jacot TA, et al. Renal expression of fibrotic matrix proteins and of transforming growth factor-β isoforms in TGF-β transgenic mice. J Am Soc Nephrol. 1999; 10:271–80. [PubMed: 10215326]
38. Wu DT, Bitzer M, Ju W, et al. TGF-β concentration specifies differential signaling profiles of growth arrest/differentiation and apoptosis in podocytes. J Am Soc Nephrol. 2005; 16:3211–21. [PubMed: 16207831]
39. Racusen LC, Monteil C, Sgrignoli A, et al. Cell lines with extended in vitro growth potential from human renal proximal tubule: characterization, response to inducers, and comparison with established cell lines. J Lab Clin Med. 1997; 129:318–29. [PubMed: 9042817]
40. Hayashida T, Jones JC, Lee CK, et al. Loss of β1-integrin enhances TGF-β1-induced collagen expression in epithelial cells via increased αvβ3-integrin and Rac1 activity. J Biol Chem. 2010; 285:30741–51. [PubMed: 20650890]

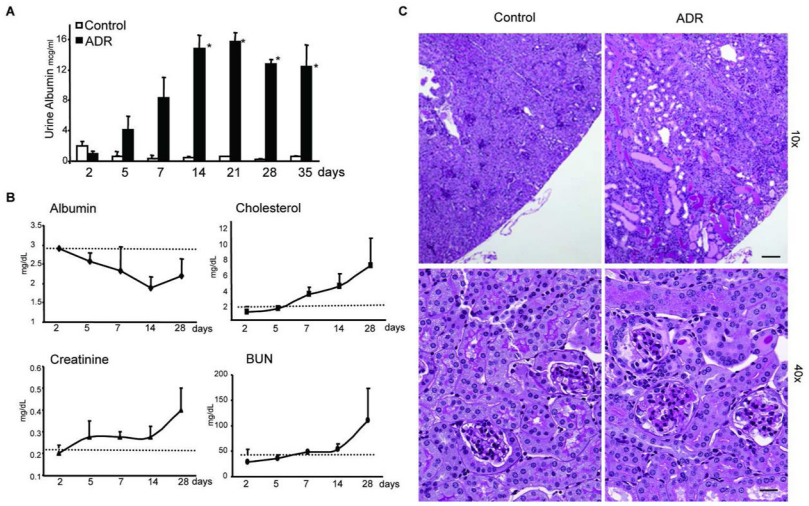

Figure 1.

Adriamycin (ADR) nephropathy in 129x1/Svj mice. 8 week-old mice received a single injection of ADR (15 mg/kg BW) or control (saline) via tail vein. *A,* At the indicated time, urine was collected for albumin determination. Proteinuria peaked at 14–21 days. ($P < 0.001$ by 2-way ANOVA comparing control vs. ADR, * $P < 0.05$ compared to control by Fisher's post hoc analyses, $N = 2 – 4$ at each time point). *B,* At the time of sacrifice, blood was collected for albumin, cholesterol, creatinine and BUN determination. The dotted horizontal lines show normal serum levels, as determined by results from control mice. The mice showed decreased albumin and increased cholesterol at 14 to 28 days. BUN and creatinine were mildly elevated at 14 days but increased further at 28 days. Statistical summary at the 2-week point is shown in Table 1. *C,* Kidney samples (day 14) were sectioned and stained using periodic-acid Schiff (PAS) and photographed at a lens objective of 10x or 40x. Scale bars = 100 μm and 25 μm, respectively. ADR mice showed focal glomerulosclerosis, crescent formation, tubular atrophy and proteinaceous material in the tubular lumen.

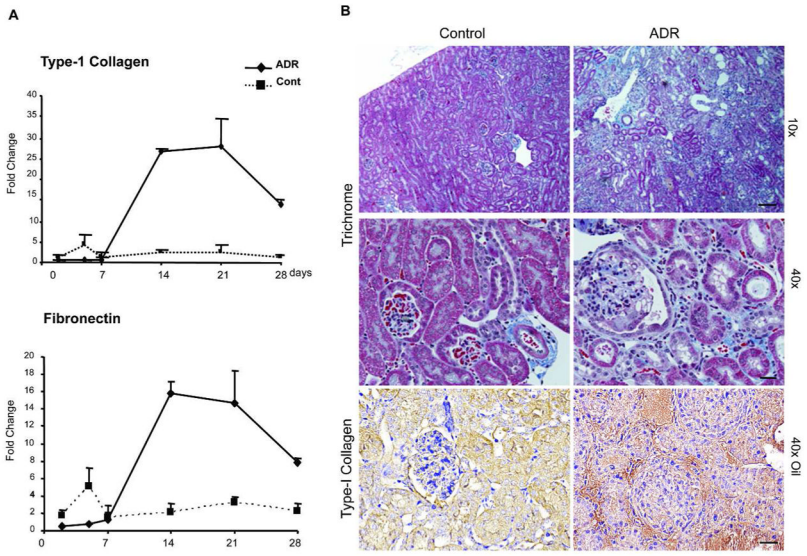

Figure 2.

Extracellular matrix accumulation in mouse ADR nephropathy. *A,* mRNA analysis by qPCR shows increased fibronectin and type-I collagen by 14 days (N = 2–4 at each time point. Statistical analyses for data at 2 weeks are shown in Figures 4B and 7A). *B,* Trichrome staining (upper panels) shows increased glomerular and tubulointerstitial accumulation of extracellular matrix. Specific staining using anti-collagen I antibody shows that type-I collagen accumulates in the glomerulus and the tubulointerstitium (bottom panels). Mice were sacrificed at day 14 after ADR administration. Scale bars = 100 μm (10x objective) and 25 μm (40x oil objective).

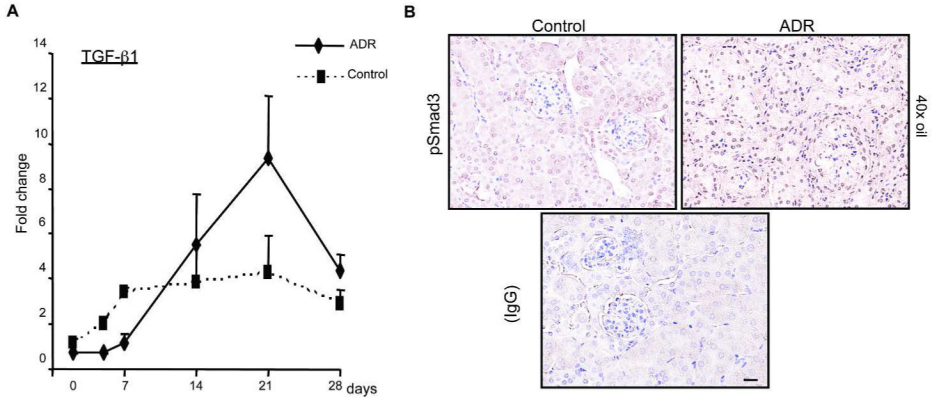

Figure 3.

TGF-β activity in the ADR-treated mouse kidneys. *A,* Quantitative PCR shows an increase in mRNA for TGF-β1 mRNA beginning at 14 days and reaching a maximum at 21 days (N = 2–4 at each time point. Statistical analyses of results at 2 weeks are shown in Figures 4B and 9B). *B,* Staining of tissue sections for phospho-Smad3 (Ser 425) shows a marked increase in nuclear staining in a kidney section from an ADR-treated mouse (day 14). Nuclear translocation of Smad3 is a hallmark of Smad3 activation. Scale bar = 25 μm.

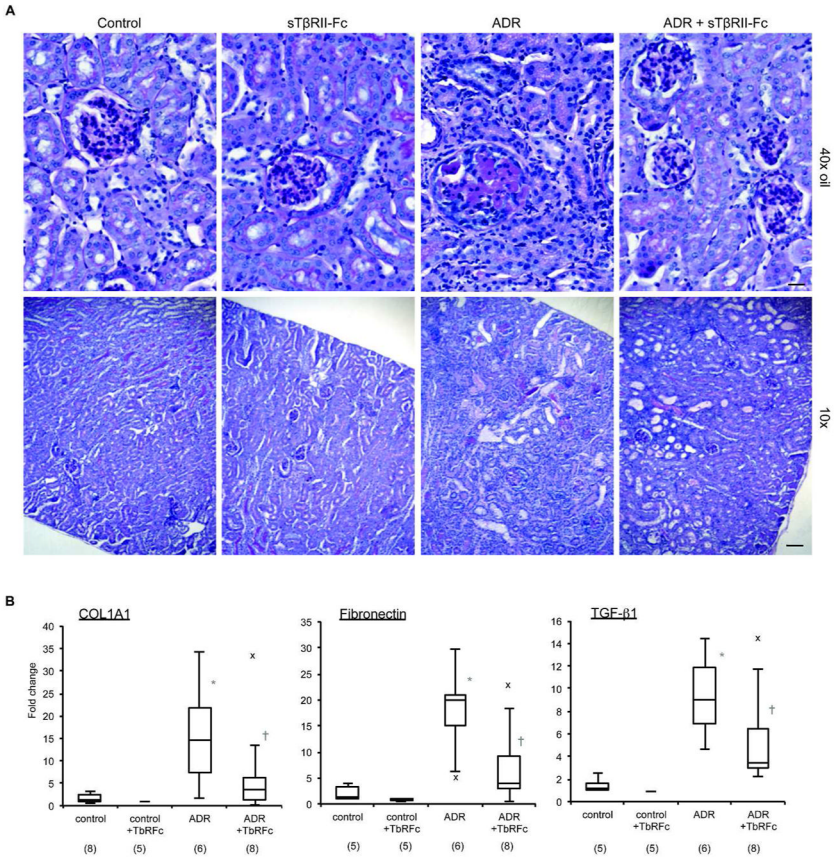

Figure 4.

Soluble type-II TGF-β receptor (sTβRII-Fc) ameliorates fibrotic changes in ADR nephropathy. ADR nephropathy was induced as described for Figure 1 and the treatment group additionally received sTβRII-Fc, 4 mg/kg via tail vein the day before ADR injection and twice a week intraperitoneally (2 mg/kg) until the conclusion of the experiment at day 14. *A,* Representative sections stained with PAS. Inhibition of TGF-β signaling improved the histological outcome of the disease. Scale bars = 25 μm (40x oil objective) and 100 μm (10x objective). *B,* sTβRII-Fc ameliorated type-I collagen, fibronectin and TGF-β1 mRNA expression induced by ADR (N shown in parentheses under each condition. COL1A1: $P = 0.019$ by 1-way ANOVA, * $P = 0.005$ compared to control, $^{\dagger}P = 0.0085$ compared to ADR; Fibronectin: $P < 0.001$ by 1-way ANOVA, * $P < 0.001$ compared to control, $^{\dagger}P = 0.0046$ compared to ADR; TGF-β1: $P < 0.001$ by 1-way ANOVA, * $P = 0.003$ compared to control, $^{\dagger}P = 0.029$ compared to ADR.

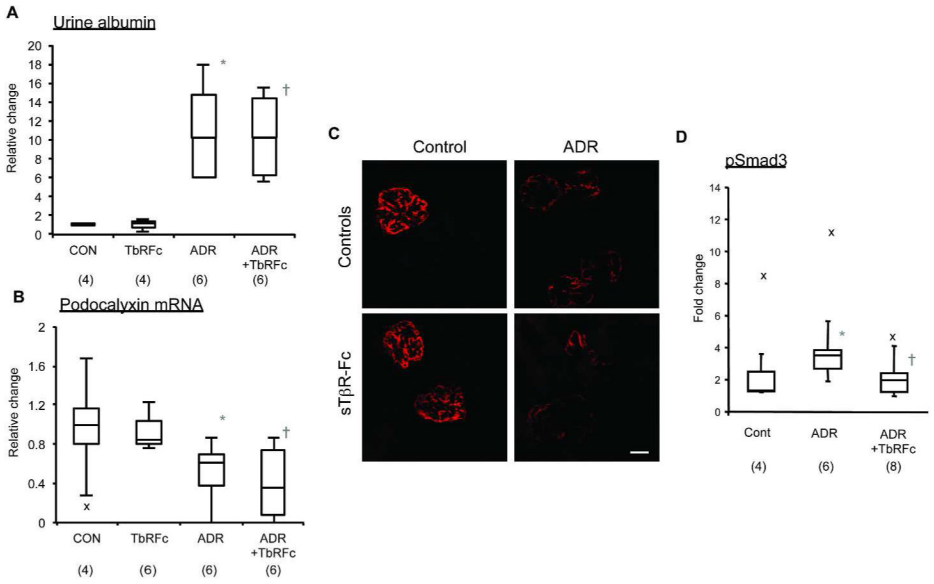

Figure 5.

Podocyte damage and proteinuria are not mediated by TGF-β. *A,* sTβRII-Fc did not decrease proteinuria (day 14; N shown in parentheses for each condition, P = 0.0016 by 1-way ANOVA, $*P = 0.0026$, $^{\dagger}P = 0.004$ compared to control). *B*, sTβRII-Fc did not prevent an ADR-stimulated decrease in podocalyxin mRNA expression (day 14; N shown in parentheses for each condition, P = 0.0016 by 1-way ANOVA, $*P = 0.0026$, $^{\dagger}P = 0.004$ compared to control). *C*, Nephirn staining was decreased at day 14 of the ADR administration even with the sTβRII-Fc treatment. 40x1.4 (Oil) objective. Scale bar = 20 μm. *D*, Smad3 phosphorylation, determined by densitometrical analyses of immunoblotting was decreased by sTβRII-Fc, confirming the efficacy of the inhibitory treatment in vivo (day 14; N shown in parentheses for each condition, P = 0.0032 by 1- way ANOVA, $*P = 0.0024$ compared to control, $^{\dagger}P = 0.027$ compared to ADR).

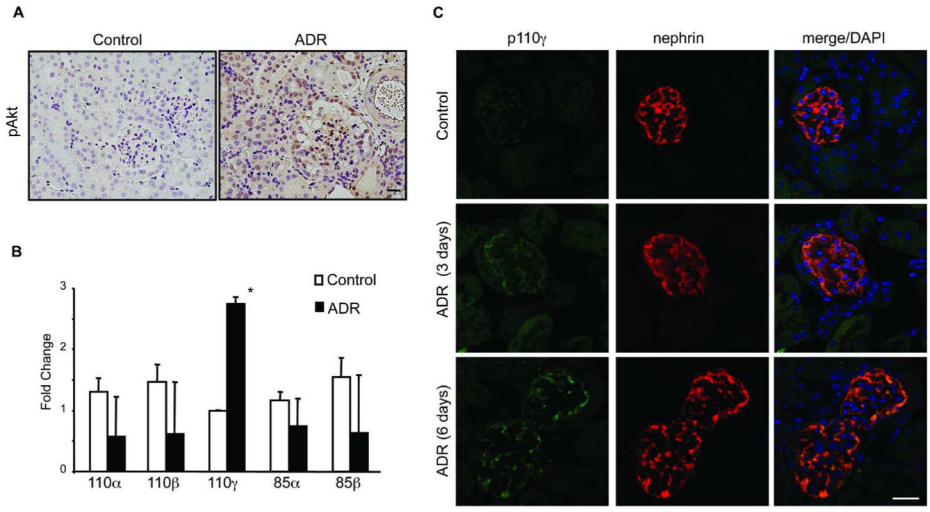

Figure 6.

PI3K γ expression is increased in ADR nephropathy. *A,* Akt phosphorylation is increased in ADR nephropathy. Tissue sections were stained with an antibody to pAkt (Ser 473). Staining is present in both nuclear and cytoplasmic patterns in ADR kidney, with particularly intense staining in glomerular nuclei. Scale bar = 25 μm. *B,* Quantitative PCR of mRNA indicates that only the 110γ subunit shows increased expression in ADR mouse kidneys (N = 4, *P < 0.05 compared to the corresponding control). p110δ was not detected. C, Immunofluorescence microscopy for p110γ and nephrin shows colocalization in a podocyte pattern. Representative images (control, day 3 and day 6 after ADR administration) of p110γ (left panels, Alexa-488 detection), nephrin (middle panels, NorthernLight detection), and merged images with nuclear co- staining (DAPI, right panels) are shown. 63x1.4 (Oil) objective. Scale bar = 20 μm

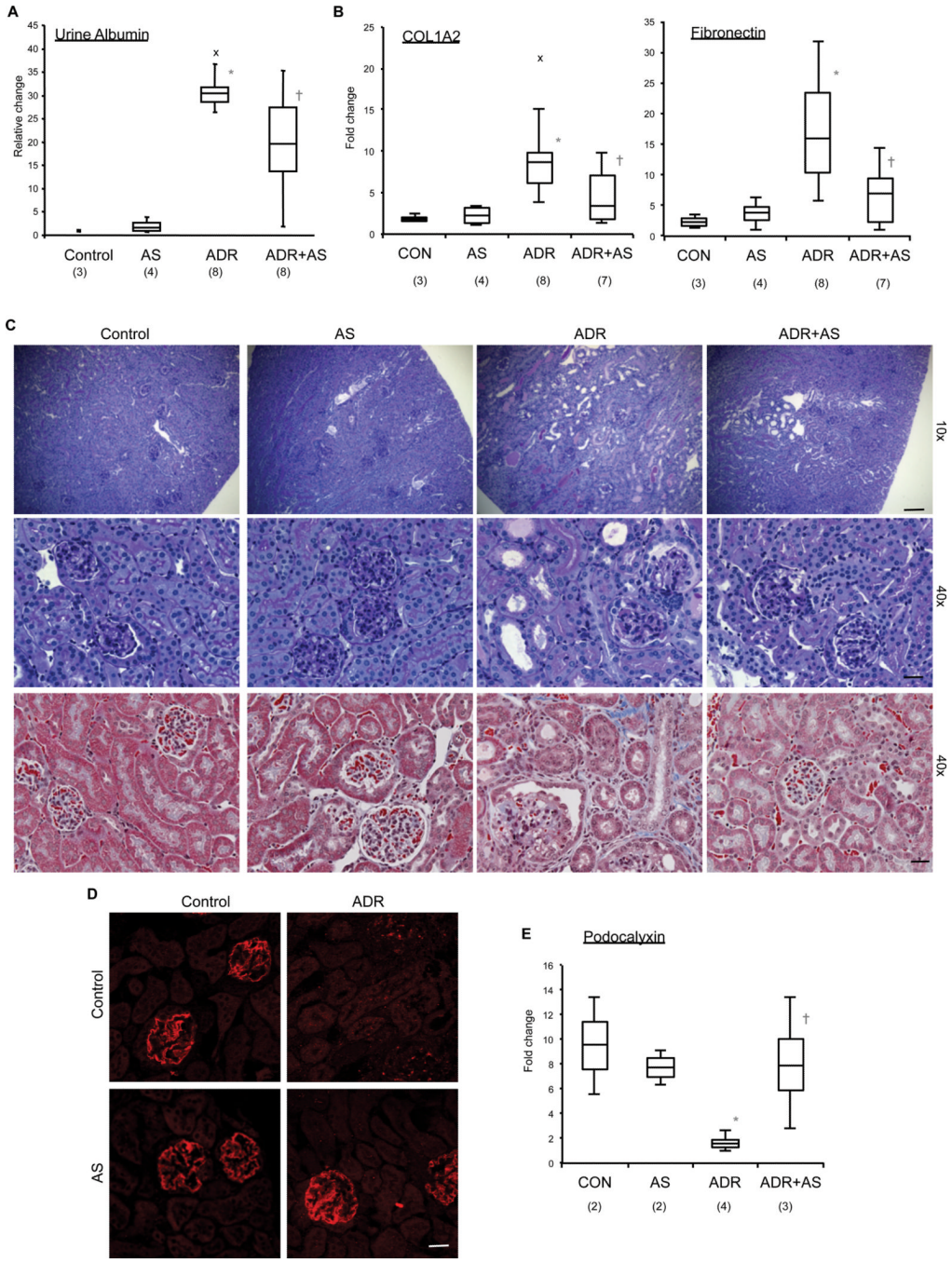

Figure 7.

Specific inhibition of p110γ prevents ADR-induced nephropathy. ADR nephropathy was induced in the presence or absence of treatment with AS605240, a biochemical inhibitor of p110γ activity (30 mg/kg, i.p.,1 day before ADR administration and every other day thereafter). *A,* Twenty-four hour urine collection was performed on day 14 after ADR administration, just prior to sacrifice of the mice. Albumin excretion was significantly ameliorated by AS treatment (N shown in parentheses under each condition. $P < 0.001$ by 1-way ANOVA, * $P < 0.001$ compared to control, $^{\dagger}P = 0.011$ compared to ADR). *B,* Type-I collagen or fibronectin mRNA expression induced by ADR, determined by qPCR, was prevented by AS treatment (day 14, N shown in parentheses under each condition. COL1A2:

$P = 0.02$ by 1-way ANOVA, * $P = 0.014$ compared to control, $^{\dagger}P = 0.035$ compared to ADR; Fibronectin: $P = 0.04$ by 1-way ANOVA, * $P = 0.029$ compared to control, $^{\dagger}P = 0.027$ compared to ADR). *C,* Sections were stained with PAS (10x objective, top panels and 40x objective, middle panels) or Trichrome (40x objective, bottom panels) staining. Scale bar = 100 μm (10x objective) and 25 μm (40x objective). AS ameliorated glomerulosclerosis, tubular atrophy and interstitial fibrosis (day 14). *D,* Glomerular nephrin, detected by immunofluorescence microscopy, is markedly decreased in ADR-treated mice, but is preserved when those mice also are treated with AS. 40x1.4 (oil) objective, scale bar = 20 μm. *E,* Podocalyxin mRNA expression, determined by qPCR, is markedly decreased with ADR treatment but is protected with AS (day 14, N shown in parentheses under each condition. $P = 0.025$ by 1-way ANOVA, * $P = 0.016$ compared to control, $^{\dagger}P = 0.008$ compared to ADR.)

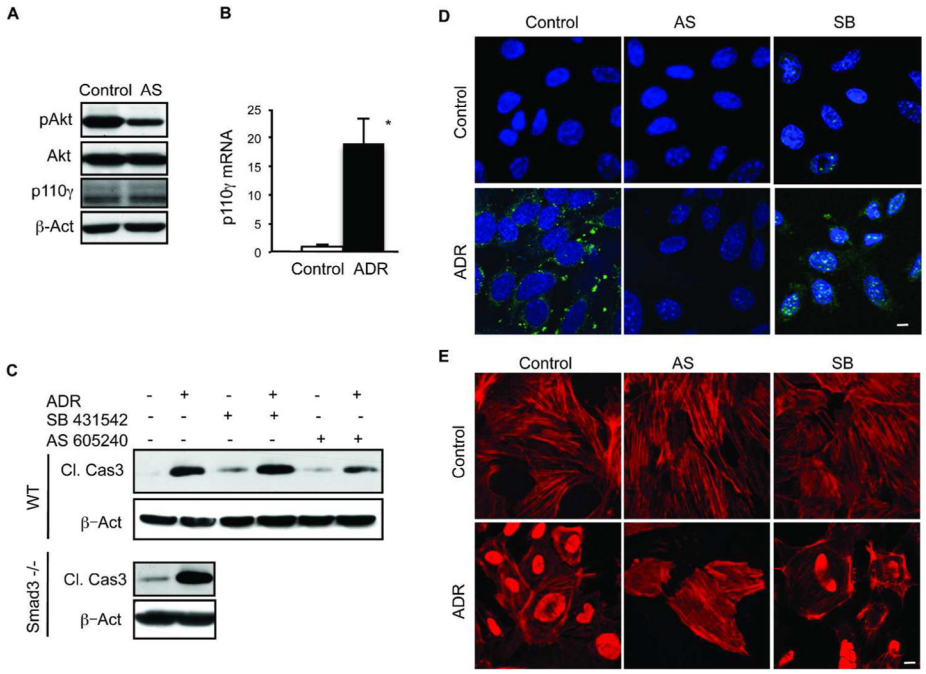

Figure 8.

p110γ expression and function in cultured podocytes. *A,* Expression and activity of the p110γ isoform in podocytes. By western blot, the protein is expressed. Akt phosphorylation, but not expression, is decreased by treatment with AS605240 (1 μM), confirming the efficacy of the inhibitor. *B,* Induction of p110γ mRNA in podocytes treated with ADR. Podocytes were cultured with and without ADR (20 μg/ml, 16 hrs) before RNA was harvested for qPCR. (N = 3, each reaction was performed in triplicate, * $P < 0.05$ compared to control). *C,* Induction by ADR of cleaved caspase 3 products in podocytes does not require TGF-β/Smad pathway. Podocytes, either wild type or Smad3 −/−, were treated with inhibitors (AS605240; AS, 1 μM, SB431542; SB, 5 μM) or vehicle for 1 hour, followed by ADR treatment (20 μg/ml, 6 hrs), and cleaved caspase 3 was detected by immunoblot. Representative blots are shown from 3 separate experiments. *D and E,* ADR induces podocyte apoptosis and cytoskeletal dysorganization in a p110γ-dependent manner. Cells were cultured with ADR (20 μg/ml) for 6 hrs following 1-hr pretreatment with either AS605240 (AS, 1 μM) or SB431542 (SB, 5 μM), and then fixed and stained with M30 CytoDEATH, a marker for early apoptosis along with nuclear DAPI staining (D) or with rhodamine-phalloidin to demonstrate actin stress fibers (E). Apoptosis marker expression and stress fiber disorganization were prevented by AS, but not by SB. 63x1.4 (oil) objective, scale bar = 10 μm.

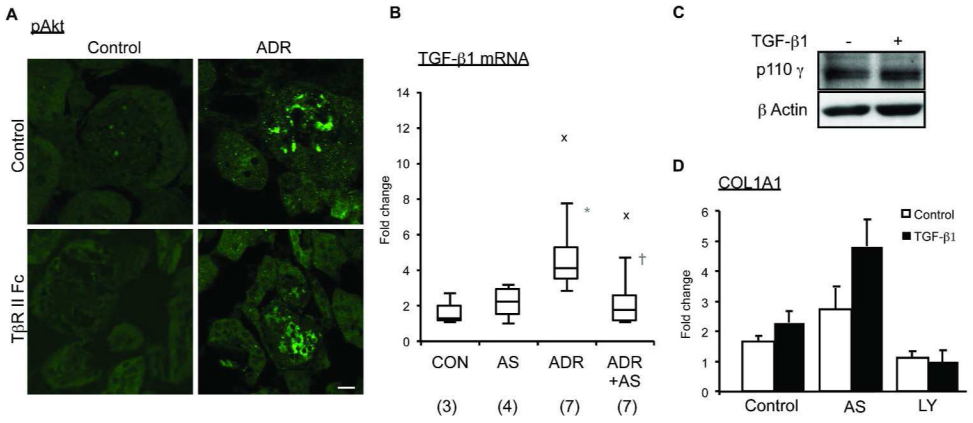

Figure 9.

Distinct roles for TGF-β and p110γ in renal cell collagen expression. *A,* pAkt activity in ADR mouse glomeruli. ADR mouse kidney samples (day 14) were stained with an antibody to pAkt. Representative images are shown. pAkt activity was present in ADR-treated glomeruli with or without sTβRII-Fc treatment, suggesting that pAkt activity is independent of TGF-β production. 63x1.4 (oil) objective, scale bar = 10 μm. *B,* Expression of TGF-βV mRNA in ADR nephropathy. TGF-β1 mRNA in mouse kidneys harvested 14 days after ADR administration was quantified by qPCR. Expression was increased by ADR treatment, an effect that was prevented in mice treated with AS605240 (N shown in parentheses under each condition. $P = 0.038$ by 1-way ANOVA, * $P = 0.02$ compared to control, $^{\dagger}P = 0.025$ compared to ADR). *C,* Effects of TGF-β on podocyte p110γ expression. Cultured podocytes were treated with TGF-βV (1.0 ng/ml, 24 hrs) or vehicle and p110γ protein levels were evaluated by immunoblotting. p110γ expression was not affected by TGF-β. Representative blots are shown from 3 separate experiments. *D,* Effect of AS on TGF-β-stimulated collagen mRNA expression. Podocytes did not produce type-I collagen in response to TGF-βV. Accordingly, the renal tubular cell line, HKC, was treated with TGF-β1 (1.0 ng/ml, 24 hrs) in the presence or absence of inhibitors and COL1A1 mRNA was determined by qPCR. AS did not prevent the collagen response, which was decreased by the pan-PI3K antagonist, LY294002 (LY, 20 μM). Representative results from one of 3 separate experiments, each performed in triplicate, are shown.

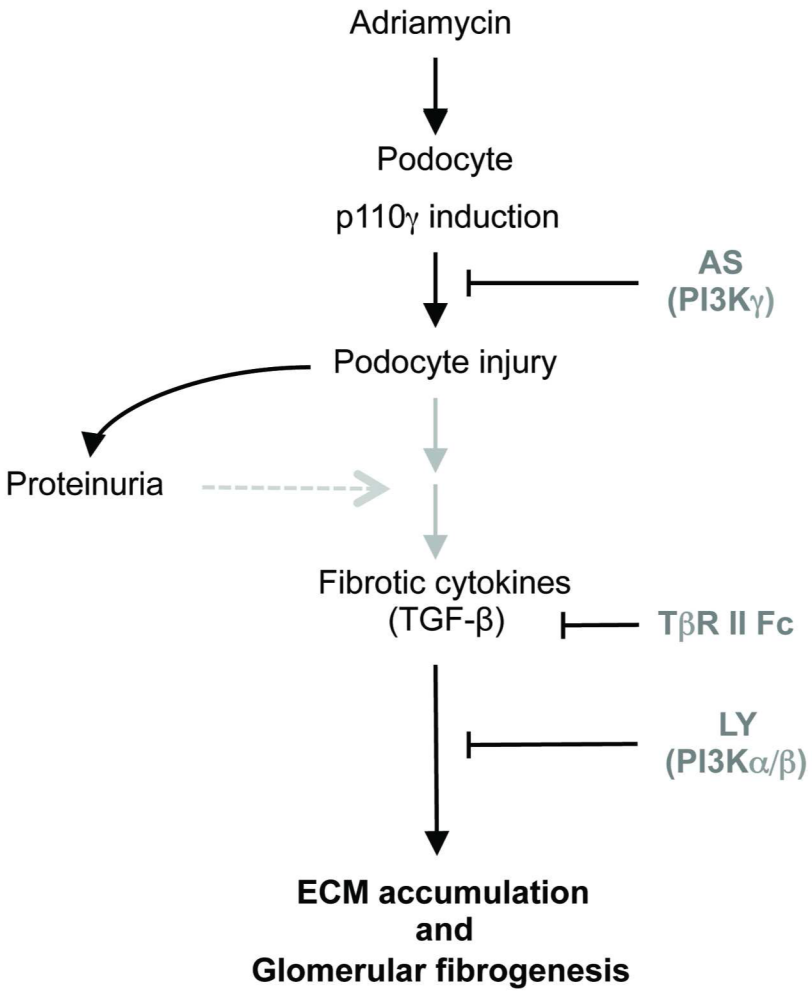

Figure 10.

Putative mechanisms by which PI3Kγ and TGF-β exert distinct effects in kidney fibrosis. Adriamycin causes podocyte injury by a mechanism that is inhibited by AS605240, indicating a role for PI3K p110γ. Subsequent, TGF-β-dependent fibrogenic activity is inhibited by sTβRII-Fc or by LY294002, but not by AS605240. These results indicate that initial podocyte injury involves the action of p110γ, whereas subsequent fibrogenesis requires TGF-β and another, non-γ isoform of PI3K.

Table 1

Nephrotic indices and kidney function of 129/SvJ mice two weeks after ADR administration.

	Albumin (g/dl)	Cholesterol (mg/dl)	BUN (mg/dl)	Creatinine (mg/dl)
Control (N)	2.8 ± 0.77 (31)	153 ± 26 (26)	37.9 ± 14.3 (31)	0.25 ± 0.07 (31)
ADR (N)	2.17 ± 0.83 (29)	410 ± 228 (28)	51.5 ± 30.7 (29)	0.27 ± 0.11 (25)
P value	0.004	<0.001	0.036	0.499

Table 2

Semi-quantitative scale of histological changes in 129/SvJ model of acquired nephropathy

Glomeruli	CONTROL	ADR	ADR + sTbeta;RII
Mesangial Hypercelluarity	0	3	0
Mesangial Matrix Expansion	0	2	0
Parietal Cell Hyperplasia	0	3	1
Focal Sclerosis	0	yes	0
Global Sclerosis	0	yes	0
Tubules			
Intraluminal Casts	0	3	2
Tubular Atrophy	0	1–2	1
Interstitium			
Inflammatory Infiltrate	0	3	1